Modeling of Dynamic Reconfiguration Performance Evaluation with State-of-Health Minded Control

Ryan Hickey, *Student Member*, *IEEE*, Christian Tigges, *Student Member*, *IEEE*, and Thomas M. Jahns, *Fellow, IEEE*

***Abstract*— Dynamic reconfiguration (DR) uses power electronic switches inside a battery pack to adaptively reconfigure the series/parallel connections of the cells, during operation, to optimize contribution to system performance. The Battery Management system implements the optimization as a function of the system operating point and each battery's present condition. Reconfiguration through State-of-Health (SOH) minded control has been investigated to evaluate the performance improvement in comparison to the traditional (e.g., static) configuration through single charge/discharge events. This study focused on understanding the performance enhancements for this reconfiguration topology over the full lifetime of the batteries. DR was shown to significantly improve performance in comparison with the static model over the systems entire lifetime, especially for systems with greater initial cell to cell variability. Further investigation was conducted to understand the performance impact relative to the number of switches, not just the maximum. Concerning performance improvement and additional cost, in most application conditions, the maximum number of switches was deemed unnecessary and less cell to cell connections can be used to minimize cost, while still maintaining the performance improvement of DR relative to the traditional static configuration.**

***Index Terms*—Dynamic Reconfiguration (DR), battery management systems (BMS), Lithium batteries, state-of-health (SOH), cell imbalance**

I. Introduction

BATTERY systems are becoming more heavily utilized in applications with overall larger cell quantities to obtain higher power and range demands [1]–[2]. While an increase in power/range is desirable, this incurs new challenges in the battery management system's (BMS) complexity from an increase in overall cell quantities, and additionally with the variation in cell to cell performance as the battery's degrade [1]–[3].

Dynamic Reconfiguration (DR) was recently proposed and investigated as a new topology to improve the system adaptability due to the nonlinear behavior of cell performance, especially in systems containing large quantities of batteries [4]–[11]. Traditional battery systems utilize fixed series-parallel connections between batteries to obtain load requirements via electrical wiring, or metal bus-bars [12]. DR systems integrate power electronic switches (e.g., MOSFET's, IGBT's) as interconnections between batteries in the system to allow real-time adjustment of cell connectivity [13].

DR's impact on performance strictly depends on the control strategy that is implemented, which is application specific. Increasing the energy density from the battery packs is largely desired, and has been researched heavily through numerous paths such as: fault tolerance [14], reduction of DC-DC converter losses through output terminal voltage matching [15], and reconfiguration based on State-of-Health (SOH) of the batteries in the system [16], [17]. This investigation will focus on SOH minded reconfiguration, as a means of improving lifetime battery and pack characteristics. Fault tolerance was studied in [14] as a way to continue operation of the battery system while minimizing the overall loss in capacity due to a failed battery. This method was shown to be an improved method than the cell level fusing that can be found in Tesla's battery pack to bypass failed batteries [18].

SOH minded reconfiguration has been previously investigated as a control methodology to increase deliverable performance to the load for DR topologies in [16], [17]. This SOH minded control focuses on reconfiguring the battery pack, while maintaining the same configuration (e.g., 2S2P), in order to deliver more energy to the load. As demonstrated in [16], [17], reconfiguring cell to cell connections to place batteries with closer levels of SOH into the same series string, can provide significantly more power capacity. In large scale battery systems, the cell performance imbalance due to nonlinear cell aging is a significant challenge for modern, static configurations to overcome [19]. Given that any given string is limited by its weakest element, integration of the DR topology with SOH minded control can provide the adaptability to handle the SOH imbalance across the cells in the battery pack, and lead to an increased deliverable performance capability.

On an operational note, the real-time estimation of the batteries individual cell SOH, which has been extensively studied previously, is essential to the successful implementation of SOH minded reconfiguration of battery packs [20], [21]. Within this investigation it will be assumed that each cells SOH can be sufficiently monitored in real time.

Battery packs contain series and parallel connections between cells in order to deliver the target output voltage and range. The series connections of the cells (e.g., cell string) results in the target output voltage of the battery pack, while the paralleled connection of cell strings increases the range, or capacity of the battery pack. Each cell string's deliverable capacity is strictly limited to the weakest cell in the string. Due to this, the cells with lower SOH's are the limiting component for deliverable performance. Reconfiguring with SOH minded control optimizes to reduce the limiting capability of the weakest cells in the system. Prior work focused on delivering more energy through SOH minded control in a single discharge event, but an understanding of how this control method effects performance through battery aging is still not understood.

This paper provides an extensive simulation analysis for

SOH minded control performance impact relative to traditional, static configuration methods as a function of key parameters discussed in Section II. After the introduction, Section II introduces the SOH minded control algorithm used, as well as the model derivation used for the analysis. The model is subsequently used to analyze the performance enhancement potential of DR compared to the static topology in Section III. Since a performance enhancement was found in Section III, further analysis on the significance of the number of Switches Per Cell (SPC) implemented in the battery pack (e.g., more switches resulting in more configuration options) effect on performance enhancement potential for the key parameters is presented in Section IV. Finally, conclusions summarizing key points are presented in Section V.

II. Simulation Model Derivation

Before introducing the structure of the simulation model, a simplified schematic is presented in Fig. 1.This schematic shows how DR fundamentally changes the battery systems circuit. In this simple example it can be seen there are two distinctly different configurations (e.g., different batteries connecting series lines), while still maintaining the same pack terminal characteristics such as terminal voltage.

This concept will remain for selecting different configurations in the more complex simulation model evaluated in this research. Connecting different batteries in series lines through SOH minded control will be compared against the standard (or static) configuration.

A. State-of-Health Minded Control Strategy

The first step in developing a control strategy based on SOH, is determining all the possible pack configuration options based on the SPC, and configuration parameter (e.g., 2S4P or 4S2P configuration). The configuration choices can be derived prior to operation of the control system, and then the controller simply needs to evaluate and select the optimum configuration in real-time. Deriving the configuration options was performed by implementing a graph theory representation similar to [15], [17] with slight changes to reflect the problem formulation for the battery aging over time. Given a battery pack, and the deliverable battery capacities at the decision time, a weighted and directed graph can be obtained as $\mathcal{G} = (\mathcal{V}, \mathcal{E}, \mathcal{W})$ such that

1. The vertex set $\mathcal{V}$ represents the batteries in the pack, denoted by $\mathcal{V} = \{b_1, b_2, \dots, b_N\}$;
2. The edge set $\mathcal{E}$ represents the configuration flexibility of the pack, e.g., which batteries can be connected to each other (SPC value);
3. The weight of each vertex is the deliverable capacity of the corresponding battery at the decision time: $\forall \omega_i \in \mathcal{W}, \omega_i = c_i (i = 1,2, \dots, N)$. The deliverable capacity is obtained by taking the battery estimated SOH at the decision time $H = \{h_1, h_2, \dots, h_N\}$ and coupling with the initial capacity for each battery $D = \{D_1, D_2, \dots, D_N\}$ to obtain $c_i (i = 1,2, \dots, N) = H \cdot D$

The configuration options found in $\mathcal{G}$ will be based on the configuration selection (4S2P, or 2S4P) as well as the configuration flexibility (SPC), resulting in a matrix of the form A_{ijk} where i corresponds to the configuration option number, j corresponds to the parallel string in the configuration, and k corresponds to the deliverable capacity of the specific battery in the series string. Application of the graph theory for the 8 cell system, the resulting number of configurations for each value of SPC can be found in Table I.

Table I: Resulting Number of Configuration Options for Each Configuration (4S2P, or 2S4P) Based on the Configuration Flexibility (SPC)

SPC	4S2P	2S4P	Total # Switches
3	1	1	23
4	4	5	30
5	21	16	37
6	32	35	44
7	35	63	51
8	35	90	58
Max	35	105	72

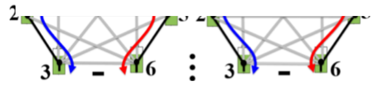

Fig. 1. Simplified schematic depicting how DR converts the standard (or static) configuration, with the schematic depicting two different configuration options from the same battery system

Table I presents the corresponding number of configurations (e.g., the number of i in A_{ijk} that will need to be evaluated) at decision time. The values of j will depend on which configuration is being simulated (j=1,2 for 4S2P and j=1,2,3,4 for 2S4P). The values of k will be the number of cells in a series string (k=1,2 for 2S4P, and k =1,2,3,4 for 4S2P). Finding the optimum configuration in A_{ijk} for this SOH minded control will be obtained by finding which configuration (e.g., which row i) results in the most deliverable energy at decision time. To obtain this, we must transform the A_{ijk} matrix from reflecting the capacities for each cell in each configuration to the total deliverable capacity of each configuration at decision time.

A_{ijk} can be transformed to a 2-Dimensional array reflecting the deliverable capacity in each series string (e.g., j) for each configuration (e.g., i) by

$$B_{ij} = \min\{A_{ijk}\} \left(k = 1,2, \dots, \frac{N}{m}\right) \quad (1)$$

where B_{ij} identifies the lowest value of deliverable capacity in each series string (e.g., each value of j) for each configuration (e.g., i) by finding the minimum value across each value of k.

As a result, the SOH minded control wants to implement the configuration with the most deliverable capacity, such that

$$\max \sum_{j=1}^{m} B_{ij} \quad (2)$$

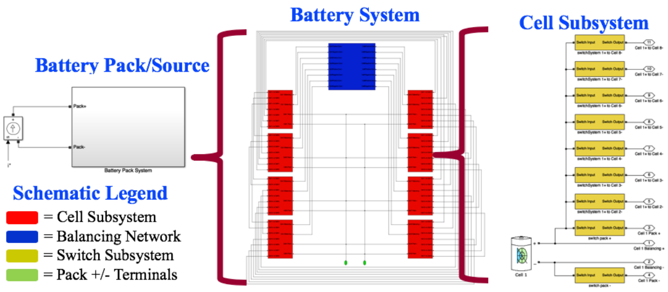

Fig. 2. Simplified model schematic for the 8 cell system

where m corresponds to the total number of parallel strings for the configuration. Implementing (2) results in the optimum configuration, at the given decision time, for the model to reconfigure to.

B. *Simulink Model Derivation*

The simulation model was derived and implemented in the Matlab Simulink environment, with utilizing the Sim Power Systems Toolbox. The goal of this research is to evaluate the performance enhancement opportunities when implementing DR and, most importantly, not to evaluate a specific battery chemistries performance. Due to this, a generic battery model was utilized that was modeled after a 2.3Ah rated cell of $LiFePO_4$ chemistry. The generic model contains an aging method, and the governing equations for the model can be found in [22]. DR should be chemistry independent, and since the same battery model was used for both the DR and the static conditions, any performance improvement can be deemed to result from the DR topology implementation. The model developed for this analysis was an 8 cell system. The overall schematic can be found in Fig. 2.

Each switch subsystems include the power electronic switches that are used for DR to connect the cell to all remaining cells in the battery pack. In the "Battery System" portion of the figure, each cell (denoted by red) contains connections to the battery pack terminals (positive and negative), the balancing network (positive and negative terminals to the resistive network), and the series connection options to the remaining cells in the battery pack. When in use for a given SPC criteria, only the switches that the controller has access to will have losses, approximated by a snubber resistance of 1mΩ. Additionally, since this analysis focuses on the battery aging, the balancing system implemented is quite important, which in this case a simple resistive balancing network was utilized.

TABLE II: TUNABLE PARAMETERS AND SPECIFICATIONS TESTED FOR EACH PARAMETER WITHIN THE SIMULATION MODEL

Parameter	Specification Tested
Pack Configuration	4S2P, 2S4P
Switches Per Cell	4, 5, 6, 7, 8, maximum
Capacity Condition	Constant, 2% Variation
SOH Condition	Constant, 2% Variation, 1(2, 3, 4, 5) Fresh amongst aged
C-Rate	5C, 2C, 1C
Simulation Type	Static, Dynamic

The tunable variables that were studied are summarized in Table II, and the parameters will be defined. The order in which these are summarized also corresponds to the order of different conditions which will be compared when studying the performance enhancement through this analysis.
A more detailed approach describes each of these parameters such that:

- Pack Configuration corresponds to the system configuration with which the simulation will be operated
- Switches Per Cell (SPC) corresponds to the number of switches implemented per cell.
- Capacity Condition corresponds to the initial condition for the cells in the battery pack. Constant corresponds to all 8 cells in the system having the exact same value, while 2% variation was a forced 2% variation (random order, normal distribution) across the 8 cells in the system.
- SOH Condition corresponds to the initial aging of the cells in the battery pack for the simulation. Constant and 2% variation here are the same as the Capacity condition. The 1(2, 3, 4, 5) fresh cells amongst aged condition corresponds to the Distributed Energy Storage (DES) case scenario presented by the sponsor company JCI, discussed in more detail later.
- C-Rate corresponds to the commanded current that will flow through each cell in the system for the simulation.
- Simulation Type corresponds to whether the model operates in the traditional static configuration (e.g., no configuration changes) or in the DR case.

III. Evaluation of Performance Enhancement via Maximum Switches Per Cell Condition

The first performance impact study involves understanding how the DR concept performs in comparison to static in the simplest form. For this the static simulations were directly compared to the DR – with max switch condition. Recall, that the max switch condition utilizes the maximum number of SPC, meaning that every battery can series connect to every battery in the system. This condition isn't practical, since as battery system's cell count increases, the needed power electronic switches increases significantly, recall Table I. However, based on the theory of this concept, this condition should show the most performance improvement which is an essential first step in understanding DR enhancements.

A. *Ideal Case – Constant initial SOH and Capacity*

The simulation results for the 8 battery system with the initial conditions for each cell set to have constant capacity and SOH, is presented below in Table III. In this case there is no variation at the start of the simulation and is thus an extremely ideal case. Many battery manufacturers, like Johnson Controls, have to "bin" sort their batteries at the plant prior to integrating into battery packs to ensure relative uniformity in a given string.

Even when mass producing, there is always a slight variation in terms of performance, actual battery capacity, and other aspects. The reason for simulating this ideal case was to understand the outcome of the DR model in a fully ideal situation as a baseline.

TABLE III: SIMULATION RESULTS FOR TOTAL ENERGY DELIVERED TO THE LOAD IN KWH UNDER CONDITIONS: 4S2P CONFIGURATION, CONSTANT SOH AND CAPACITY FOR INITIAL CONDITIONS, 30MV BALANCING TOLERANCE, AND DR MAX CONFIGURATION OPTIONS

Model	5C-Rate	2C-Rate	1C-Rate
Static	84.834	131.368	191.004
Dynamic	84.363	129.7547	186.8526

Initial examination of results shows that, in all C-Rates tested, the static model delivered more energy to the load than the DR – max condition case. At first, this may be troublesome, as DR would be expected to outperform the static configuration. However, by adding large amounts of switches, the amount of losses increases as well. Remember that in order for the DR case to outperform the static case it must deliver enough extra energy to counteract the newly introduced switching losses. The way that DR extends performance is by changing the configuration to a better configuration option at any given time. In this simulation case, all of the cells start with the same aging and capacity, so in order for a new configuration to be selected by the controller, the cells need to age nonlinearly to a point where the same configuration is no longer best.

The average cell energy per cycle across the 8 cell system for the simulated ideal case is shown in

Fig. 4. Error bars are shown to display the standard deviation across the 8 cells in the system.

In each of the 3 C-Rate cases, the DR simulations show a sudden increase in energy per cycle around ¾ of the total simulation time for that respective C-Rate. This sudden increase shows the critical point for the DR case, where the batteries in the system nonlinearly aged enough to result in a new configuration being optimal. Additionally, it seems as though the separation between static and DR increases past this point for lower C-Rates.

B. Practical Case – 2% variable initial SOH and Capacity

The next logical step is to explore the practical cases with cell variation resulting from "bin" sorting. This variation will pair better with DR allowing the performance increase to outpace the losses caused by the additional switches. Table IV shows the more practical simulation results, for total energy delivered to the load, when inducing a 2% variation in both SOH and capacity across the eight cells in the system. When inducing this more practical initial aging and capacity, the DR delivers more energy to the load across all 3 C-Rates. Now that the system has more cell variability, the DR controller is able to find more optimized configurations and is able to execute the DR topology to begin improving performance earlier in the simulation. The DR case showed a 3.07% improvement for the 5C-Rate condition, 3.39% improvement for the 2C-Rate condition, and 1.23% improvement for the 1C-Rate condition.

Similar to the ideal case, Fig. 3 shows the average and standard deviation for the 8 cells in the system is shown for the energy per cycle, but now corresponding to the practical case. A couple observations can be made from this figure. First, the error bars are significantly reduced for the DR condition relative to the static condition for each respective C-Rate. Secondly, the performance separation for the DR case to the

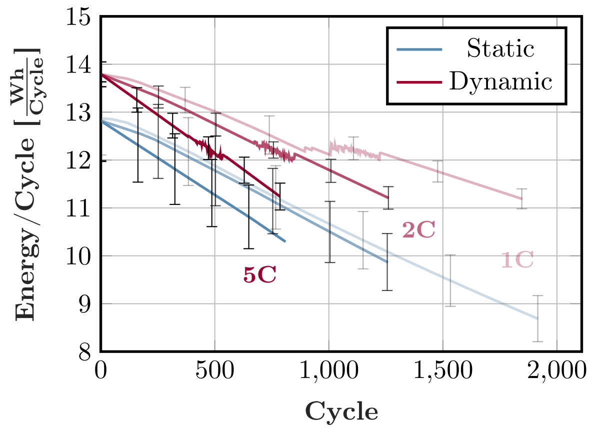

Fig. 3 Average cell energy per cycle for the practical case

0 500 1,000 1,500 2,000

Cycle

Fig. 4 Average cell energy per cycle for the ideal case

static case increases more significantly for each C-Rate in comparison to the ideal case. Lastly, the critical point where the DR topology begins improving performance is much sooner than in the ideal case.

Since both the deliverable energy, and the cell energy showed significant improvement for the DR topology in this more practical case, further analysis to understand where the performance improvement came from was performed.

Fig. 5 shows the configuration choice throughout the simulations for the DR case, where (a) corresponds to the ideal case simulation, and (b) corresponds to the practical case simulation. There are two important observations to make from this figure. The first, is the total number of switch events (e.g., reconfigurations) denoted in each figure. The ideal case has 2,497 switching events, where the more practical case increases significantly to 3,345 switching events. Recall, that the static configuration remains in the first configuration the entire time, so in both cases, the DR topology finds more than 2,400 instances where a better configuration exists, but in order to overcome the losses induced from the additional switches, the switching events needs to be increased beyond the ideal case. Lastly, the time denoted in each figure where the 1st reconfiguration takes place is critical to understanding the performance enhancement in the practical case compared to the ideal case. The ideal case reconfigured starting at around 180 hours of simulation time, while the practical case began

TABLE IV: SIMULATION RESULTS FOR TOTAL ENERGY DELIVERED TO THE LOAD IN KWH UNDER CONDITIONS: 4S2P CONFIGURATION, 2% VARIABLE SOH AND CAPACITY FOR INITIAL CONDITIONS, 30MV BALANCING TOLERANCE, AND DR MAX CONFIGURATION OPTIONS

Model	5C-Rate	2C-Rate	1C-Rate
Static	77.7633	122.7648	182.7275
Dynamic	77.9582	127.3728	185.1912

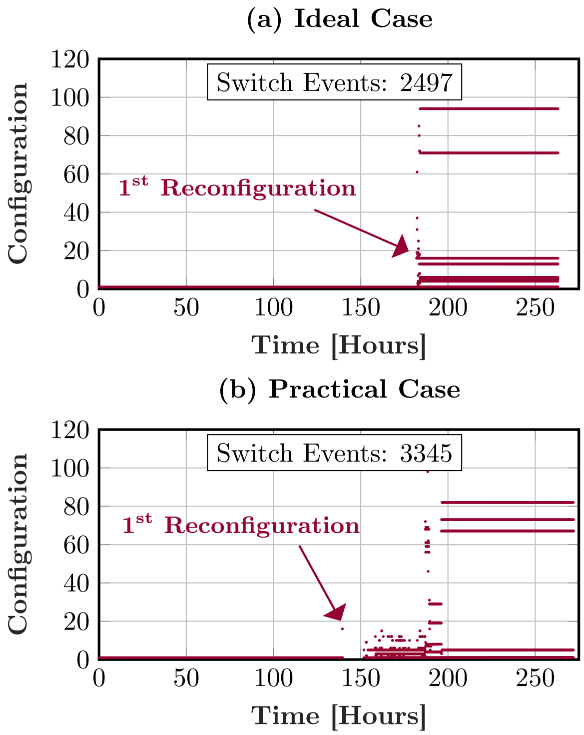

Fig. 5 Configuration choice where (a) shows the ideal case simulation, and (b) shows the practical case simulation

reconfiguring around 140 hours of simulation time. This additional 40 hours of reconfiguring time turned the DR system from under-performing the static topology (in the ideal case) to outperforming the static topology (in the practical case).

While the DR topology in the practical case certainly improved performance beyond the static topology, the DR model did not begin reconfiguring until halfway through the battery systems lifetime. This means, that for systems with larger cell variance (e.g., capacity or SOH), the DR would be able to reconfigure immediately which in theory would significantly boost the performance.

The final metric analyzed for this practical case was the final SOH of the batteries in the system for both the static and DR topologies. Recall, the failure criteria (e.g., end of the simulation) occurs when one of the 8 cells in the system reaches 80% SOH. Ideally, all of the batteries would reach 80% at the exact same instant, but due to nonlinear aging of batteries, this wouldn't happen in the static topology. However, by reconfiguring with SOH minded control, better utilization of the batteries occur, which should result in reducing the average SOH of the batteries when the simulation ends. Table V shows the final SOH values, both mean and standard deviation, across the 8 cells in the system for each of the C-Rates simulated. Note that in all C-Rate cases, the DR model results in lower mean and standard deviation values of SOH. Due to this, the DR model clearly better utilizes the capability of the batteries in the system, which ultimately lead to outperforming the static topology in this more practical case.

TABLE V: FINAL CELL SOH FOR THE PRACTICAL CASE, WITH MEAN AND STANDARD DEVIATION SHOWN ACROSS THE 8 CELLS IN THE SYSTEM

Model	5C-Rate		2C-Rate		1C-Rate	
	Mean	**St.Dev.**	**Mean**	**St.Dev.**	**Mean**	**St.Dev.**
Static	82.0	1.913	81.9	1.738	82.8	2.237
Dynamic	81.3	1.234	80.9	1.114	81.2	0.948

The initial results comparing static to the DR – max switch conditions, show that increased cell variability results in better performance for the DR topology. This will guide the continued study within this paper to see how far this benefit goes compared to increased cell variability. This increase in performance with cell variability is particularly beneficial in a practical case. In production, significant effort is put forth to reduce this variability, since it is a significant hinderance in any static system. With DR, cells with widely difference characteristics could be put together in a pack and still be fully utilized. The use of DR could mean a relative end or at least significant reduction in bin sorting, two-fold reducing the cost of production and increasing pack performance.

IV. Parameter Effect on Performance Improvement Opportunities

The priority of this investigation was to understand if DR performance improvements were only evident in the maximum SPC configuration. This investigation runs separate simulations for multiple SPC criteria, ranging from 4 through 8. It also includes the static and max switch conditions for comparison. Recall, that all switches have 2 dedicated to the pack parallel connections, and the remaining switches were used for series connections with other batteries.

A. Distributed Energy Storage Comparison

Prior sections showed that by inducing more variance into the system (ideal case to practical case), the performance enhancement of DR became more evident. Consultation with our sponsor company (Johnson Controls) introduced the Distributed Energy Storage (DES) scenario, where a battery system consists of many modules, where the modules would contain a battery pack of cells. In this application, a cell in the module would fail, and due to cost concerns, the entire module would be replaced with a new, or fresh module, rather than open the module and find/replace the failed cell. Due to this implementation of fresh modules amongst previously used modules within the battery system, a DES case was investigated to understand if DR can better utilize the batteries when fresh modules are placed with previously (e.g., aged) modules.

As time goes by, more and more fresh modules are placed amongst the aged ones, which is the fundamental reason that numerous simulations were conducted to understand the DR performance enhancement when implementing anywhere from 1-3 fresh cells amongst the remaining cells in the 8 cell battery pack. Simulation results for the percent improvement (of energy delivered to the load) of DR topologies compared to the static topology for each of the DES cases are shown in Fig. 6. A few observations can be made from this figure regarding DR performance enhancement. First, in all cases (C-Rate, SPC), the DR outperforms the static topology. Lastly, the performance enhancement certainly is dependent on the number of switches

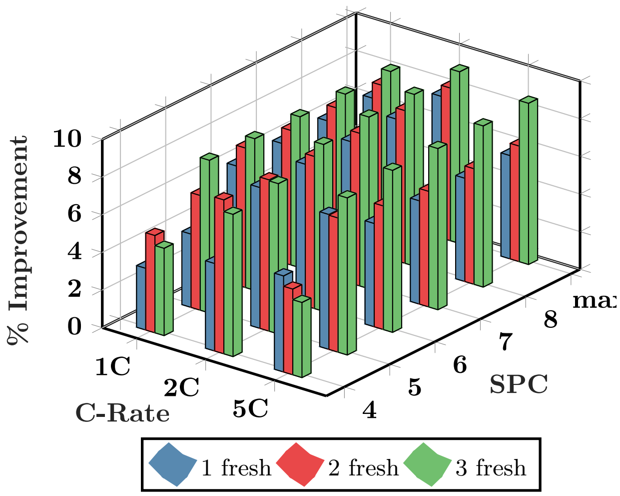

Fig. 6 Percent improvement for energy delivered to the load of DR (various SPC) cases compared to static as a function of the initial condition DES case (1, 2, 3 fresh cells)

implemented. The SPC of 4 shows lower performance enhancement compared to the rest, however, it should be noted that it still improves the deliverable energy compared to the static model. Although, the performance enhancement seems to saturate, providing the indication that the additional switches needed for the higher values of SPC might be cost inefficient, and unnecessary to provide the same performance attributes.

While the performance enhancement is certainly a desired attribute, previous sections identified DR as a means of reducing the cell to cell performance variation by better utilizing the cells in the system. The standard deviation values across the 8 cells in the system for the DES cases of 1-3 fresh cells is show in Table VI. First, the DR topology certainly does reduce the standard deviation in comparison to the static case for each of the C-Rates, and DES conditions. Additionally, the standard deviation seems to saturate around SPC values of 7, which indicates that the additional switches needed for SPC 8 and SPC max are unnecessary and can be eliminated to reduce overall system cost. This again indicates that cost reduction can be performed in a commercial application setting to reduce the number of switches in the system (e.g., reducing material costs) while still maintaining the same performance enhancement.

The SPC didn't show quite the variation for the delivered energy, but further investigation was performed to identify where the additional SPC values provide performance

Table VI: Standard deviation values across multiple C-Rates and SPC for the cell energy comparison of 1-3 fresh cells in the 8 cell system

		5C-Rate		
Model	**SPC**	**1 Fresh**	**2 Fresh**	**3 Fresh**
Static	-	0.0955	0.0971	0.095
Dynamic	4	0.0078	0.0451	0.0485
	5	0.0721	0.0736	0.1016
	6	0.0468	0.0707	0.1073
	7	0.0468	0.0596	0.0950
	8	0.0468	0.0596	0.0950
	Max	0.0468	0.0596	0.0950
		2C-Rate		
Model	**SPC**	**1 Fresh**	**2 Fresh**	**3 Fresh**
Static	-	0.1403	0.1437	0.1390
Dynamic	4	0.0101	0.0904	0.1415
	5	0.1493	0.0949	0.1390
	6	0.0707	0.0931	0.1738
	7	0.0707	0.0899	0.1444
	8	0.0707	0.0899	0.1444
	Max	0.0707	0.0899	0.1444
		1C-Rate		
Model	**SPC**	**1 Fresh**	**2 Fresh**	**3 Fresh**
Static	-	0.1718	0.1813	0.1695
Dynamic	4	0.0917	0.2336	0.3054
	5	0.3406	0.1440	0.2468
	6	0.0997	0.1241	0.2311
	7	0.0997	0.1249	0.2081
	8	0.0997	0.1249	0.2081
	Max	0.0997	0.1249	0.2081

enhancement. Fig. 7 shows the average cell energy throughput of the 8 cells in the system for each of the DES cases. Combining the results from this figure for the average energy throughput, along with the results in Table VI for the standard deviation results, the performance impact of the value of SPC can be better depicted. Understanding the performance difference from the delivered energy was insignificant, but understanding how the cell to cell variation in performance (average values through this figure, and variance through the table), gives better insight into how the values of SPC effect performance. In this case, the lower values of SPC show higher cell to cell variance throughout the simulation, but by adding

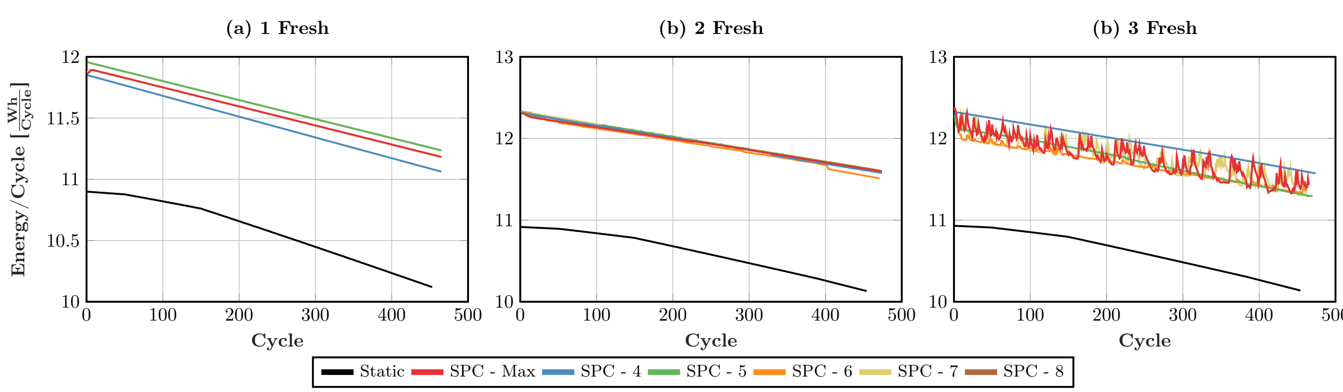

Fig. 7 Simulation results for the average cell energy throughput across the 8 cells in the system for the DES cases, where (a) 1 fresh, (b) 2 fresh, and (c) 3 fresh cells are in the battery pack

Table VII: Standard deviation values across multiple C-Rates and SPC for the cell energy throughput comparison for 4S2P and 2S4P configurations in the 8 cell system for the DES - 1 fresh case

Model	SPC	5C-Rate		2C-Rate		1C-Rate	
		4S2P	2S4P	4S2P	2S4P	4S2P	2S4P
Static	-	0.096	0.136	0.140	0.201	0.172	0.2523
Dynamic	4	0.008	0.067	0.010	0.100	0.092	0.133
	5	0.072	0.082	0.149	0.119	0.341	0.163
	6	0.047	0.082	0.071	0.119	0.099	0.163
	7	0.047	0.055	0.071	0.085	0.099	0.121
	8	0.047	0.055	0.071	0.085	0.099	0.120
	Max	0.047	0.055	0.071	0.085	0.099	0.120

the extra expense for more switches (e.g., moving to higher values of SPC), the cell to cell variance is significantly reduced, but also more consistent throughout the battery systems lifetime.

This DES case provided by Johnson Controls has shown to be a niche area for DR topologies to thrive. The performance enhancement relative to the static configuration has shown to drastically increase performance in this scenario. This investigation validated the necessity for system variance in order to fully maximize the potential of DR technology. By reducing, or ultimately mitigating the bin sorting process, DR would show the ability to overcome the cell to cell variance, while still maximizing the deliverable performance demanded by applications. Additionally, as cells in the system are aged, DR has shown the ability to adapt in real time to better utilize the remaining energy, thus boosting performance in addition to extending the overall lifetime of the battery system.

B. Configuration Comparison

The last investigation will focus on the effect of the battery pack configuration as well, where previous sections focused solely on a single configuration (4S2P), or solely the maximum SPC condition. Since the simulation model is a 8 cell system, this investigation will compare the only two potential configurations: 4S2P, and 2S4P. Note, that 1S8P and 8S1P are alternative configuration topologies, but the cell order in these is irrelevant, so DR cannot change anything. Additionally, the DES – 1 fresh case will be used for the initial conditions, as this test condition showed the most promise for DR topologies in previous sections.

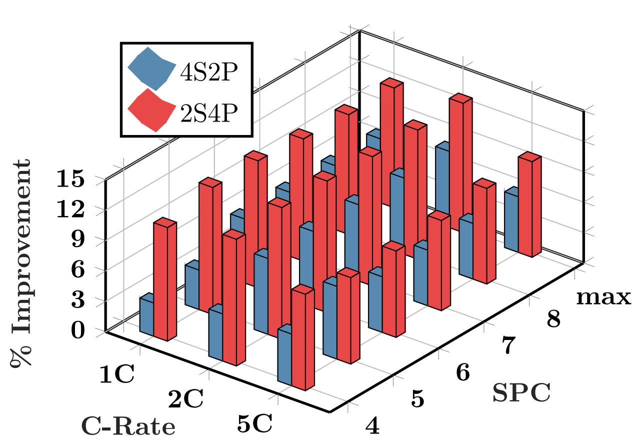

Fig. 9 Simulation results for % improvement for deliverable energy to the load of DR topology to static topology for DES - 1 fresh test case displaying both configurations

Fig. 9 shows the simulation results for the percent improvement of each DR case (where one axis shows the SPC value, and the percent improvement Z-axis relates the improvement from that SPC value to the static case) for the total energy delivered to the load. Note that in all cases, the percent improvement for energy delivered to the load was increased for the 2S4P configuration in comparison to the 4S2P configuration. This means, that by increasing the number of parallel strings in the system, the DR performance enhancement potential increases. Further investigation was performed to evaluate the cell to cell variation in performance, in terms of cell energy throughput, for each of the C-Rates, and Configuration topologies. Table VII shows the cell to cell standard deviation across the 8 cell system, for both the static topology, and each of the SPC simulated DR topologies. Note, that in most cases, the DR topologies have lower standard deviations, which is desired. However, it is important to note that in some SPC cases, the static model has lower standard deviation, proving the case for the need to implement additional switches (with additional cost and system complexity), in order to obtain all around improved performance. Additionally, note that in both the static and DR cases, by increasing the number of parallel strings, the standard deviation across the 8 cells in the system increases. However, in the DR cases, the standard deviation is largely reduced, which can result in better lifetime

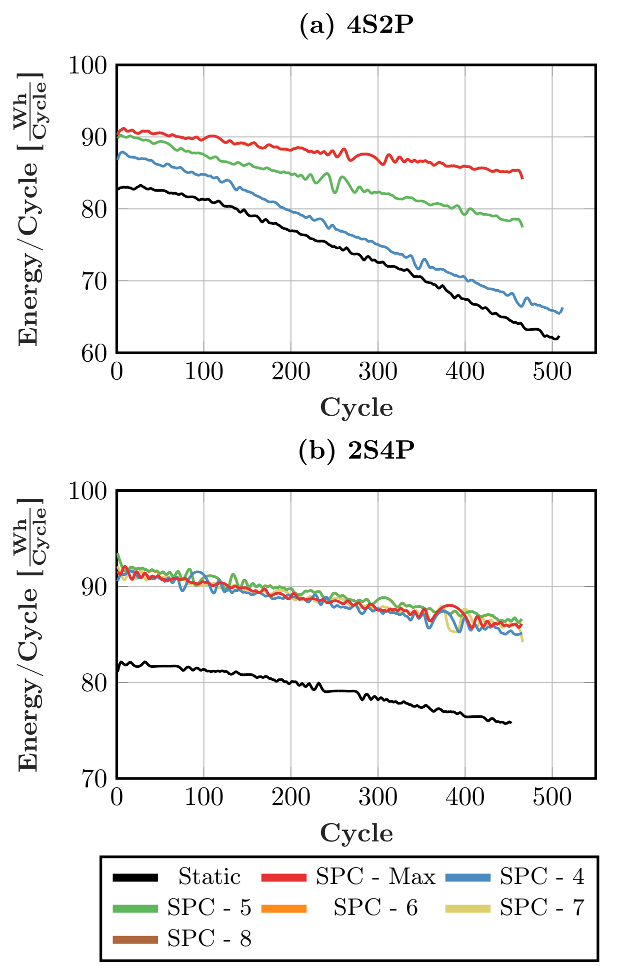

Fig. 8 Simulation results for energy delivered to the load per cycle for 1C-Rate, under initial conditions of DES - 1 fresh case, where the results are shown for (a) 4S2P configuration, and (b) 2S4P configuration

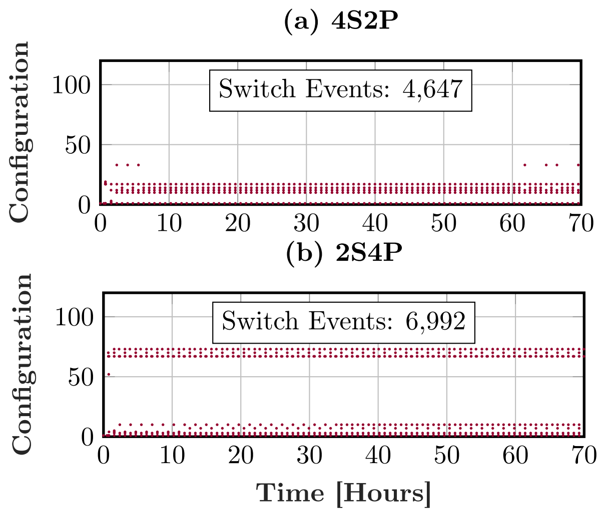

Fig. 10 Configuration choice for the DES - 1 fresh case comparing the battery pack configuration, where (a) 4S2P configuration, and (b) 2S4P configuration

predictability, and range prediction in real world applications. Further investigation was conducted to evaluate the performance differences for each of the SPC values within the DR topologies.

Fig. 8 shows the 1C-Rate simulation results for delivered energy to the load per cycle for the static and DR (each SPC value shown separately), where (a) corresponds to the 4S2P configuration, and (b) corresponds to the 2S4P configuration. This figure depicts the simulation results for the DES case previously discussed, where the DR topology has been shown to provide the most significant performance improvement, this demanding further research investigation for potential commercial application deployment. Examining this figure, the first observation should be that for lower numbers of parallel strings (e.g., 4S2P configuration), the SPC has much larger effect on the performance improvement. However, for higher values of parallel strings (e.g., 2S4P configuration), the various SPC values seemingly have no effect on the performance improvement of DR. This is important to understand, as in applications with larger quantities of parallel strings, the additional cost of switches, as well as controller complexity is seemingly unnecessary to obtain the same performance improvement of DR.

Increasing the number of parallel strings has shown to allow DR performance improvement to increase significantly. Fig. 10 shows the configuration selection throughout the entire simulation for (a) the 4S2P configuration, and (b) the 2S4P configuration. A few observations should be made from this figure. First, by increasing the number of parallel strings, the overall reconfiguration opportunities significantly increases from 4,647 to 6,992. Additionally, note that the static configuration remains in the same configuration the entire simulation, and in each of these configuration cases, the controller found thousands of opportunities where the initial configuration was not the optimal case. Secondly, by examining each of the configuration choice figures, the reconfiguration controller seems to gravitate towards a small percentage of configurations throughout the lifetime of the system. This is important, since as the cell count in the battery system increases, the number of overall configurations increases quite significantly. If in these cases, majority of the configurations are not necessary to maintain the DR performance improvement, they can simply be left out of the reconfiguration controller, allowing the evaluation of determining the optimal configuration to be performed more rapidly.

Studying the different SPC criteria and pack configuration types bring up important engineering conclusions looking at the benefits and drawbacks of DR. First and foremost, the max SPC condition is not necessary for significantly improved results. In this 8 cell system using the 4S2P configuration the improvement begins to plateau at an SPC of 7, using 29% less switches. Furthermore, SPC performance differences are more significant for lower parallel strings, if increasing parallel strings, cost reduction of the system can be obtained with lower SPC values, while maintaining the same performance enhancement.

V. Conclusions

A promising simulation model utilizing a Lithium-Ion battery aging model was utilized to evaluate unique parameter effects on performance output when integrating the DR topology throughout a battery energy storage system. The impact of pack configuration, C-Rate, initial aging (e.g., SOH) and Capacity, and the significance of SPC were considered on the resulting impact on DR performance improvement relative to the traditional-static configuration. Key conclusions from this paper include:

- At the fundamental level, integrating DR topology into a battery system results in a performance improvement for deliverable energy in comparison to a traditional (static) topology.
- The resulting value of SPC has a significance on the performance improvement, however, a optimization can be performed when the application specific criteria is known to reduce cost of DR integration by reducing the value of SPC.
- The SOH minded reconfiguration showed to reduce the cell to cell variability in cell energy throughput across the cells in the system throughout the battery systems lifetime, thus showing better overall battery utilization.
- Increasing the number of parallel strings in the system resulted in increased performance improvement with DR, additionally resulting in lower significance for the value of SPC on performance improvement in systems with higher numbers of parallel strings.

The insight from this simulation model is expected to help guide future research for in lab experiments that require significant more of a time commitment.

Acknowledgment

The authors thank Johnson Controls-Power Solutions and the Wisconsin Electric Machines and Power Electronics Consortium (WEMPEC) for their support.

References

[1] "The Composition of EV Batteries: Cells? Modules? Packs? Let's Understand Properly!" [Online].

Available: https://www.samsungsdi.com/column/technology/detail/54344.html?pageIndex=1&idx=54344&brdCode=001&listType=gallery&searchKeyword=. [Accessed: 12-Dec-2018].

[2] "BU-1003: Electric Vehicle (EV) – Battery University." [Online]. Available: https://batteryuniversity.com/learn/article/electric_vehicle_ev. [Accessed: 27-Aug-2018].

[3] H. Kim and K. G. Shin, "Dependable, Efficient, Scalable Architecture for Management of Large-scale Batteries," 2018.

[4] T. Kim, W. Qiao, and L. Qu, "Power Electronics-Enabled Self-X Multicell Batteries: A Design Toward Smart Batteries."

[5] S. Ci, J. Zhang, H. Sharif, and M. Alahmad, "Dynamic reconfigurable multi-cell battery: A novel approach to improve battery performance," *Conf. Proc. - IEEE Appl. Power Electron. Conf. Expo. - APEC*, pp. 439–442, 2012.

[6] T. Kim, W. Qiao, and L. Qu, "Series-Connected Self-ReconfigurableMulticell Battery."

[7] D. Raychev, Y. Li, and W. Shi, "The Seventh Cell of a Six-Cell Battery."

[8] E. Kim, K. G. Shin, and J. Lee, "Modeling and Real-Time Scheduling of Large-Scale Batteries for Maximizing Performance," *Proc. - Real-Time Syst. Symp.*, vol. 2016–Janua, pp. 33–42, 2016.

[9] S. Steinhorst *et al.*, "Distributed reconfigurable Battery System Management Architectures," *Proc. Asia South Pacific Des. Autom. Conf. ASP-DAC*, vol. 25–28–Janu, pp. 429–434, 2016.

[10] L. He, L. Kong, and S. Lin, "RAC : Reconfiguration-Assisted Charging in Systems, Large-scale Lithium-ion Battery," vol. 7, no. 3, pp. 1420–1429, 2016.

[11] S. Ci, N. Lin, and D. Wu, "Reconfigurable Battery Techniques and Systems: A Survey," *IEEE Access*, vol. 4, pp. 1175–1189, 2016.

[12] "Serial and Parallel Battery Configurations and Information." [Online]. Available: https://batteryuniversity.com/learn/article/serial_and_parallel_battery_configurations. [Accessed: 13-Dec-2018].

[13] F. Baronti, G. Fantechi, R. Roncella, and R. Saletti, "Design of a module switch for battery pack reconfiguration in high-power applications," *IEEE Int. Symp. Ind. Electron.*, pp. 1330–1335, 2012.

[14] H. Kim and K. G. Shin, "On dynamic reconfiguration of a large-scale battery system," *Proc. IEEE Real-Time Embed. Technol. Appl. Symp. RTAS*, pp. 87–96, 2009.

[15] L. He, L. Gu, L. Kong, Y. Gu, C. Liu, and T. He, "Exploring adaptive reconfiguration to optimize energy efficiency in large-scale battery systems," *Proc. - Real-Time Syst. Symp.*, pp. 118–127, 2013.

[16] L. He, Y. Gu, T. Zhu, C. Liu, and K. G. Shin, "SHARE: SoH-Aware Reconfiguration to Enhance Deliverable Capacity of Large-Scale Battery Packs," *Proc. ACM/IEEE Sixth Int. Conf. Cyber-Physical Syst. - ICCPS '15*, pp. 169–178, 2015.

[17] L. He, Z. Yang, Y. Gu, C. Liu, T. He, and K. G. Shin, "SoH-Aware Reconfiguration in Battery Packs," *IEEE Trans. Smart Grid*, vol. 9, no. 4, pp. 3727–3735, 2018.

[18] "EP 2 416 405 A1 EUROPEAN PATENT APPLICATION," 2011.

[19] F. Jin and K. G. Shin, "Pack Sizing and Reconfiguration for Management of Large-scale Batteries."

[20] J. L. Vian, "(12) United States Patent45) Date of Patent: (54) (75) (73) (*) (21) (22) (65) (51) (52) (58) HEALTH MANAGEMENT OF RECHARGEABLE BATTERIES," 2014.

[21] Davide Andrea, *Battery Management Systems for Large Lithium Ion Battery Packs - Davide Andrea - Google Books*. 2010.

[22] Mathworks, "MathWorks Battery Model," 2018. [Online]. Available: https://www.mathworks.com/help/physmod/sps/powersys/ref/battery.html.